Thermal Sensation Study of Wooden Desktop Based on COMSOL Multiphysics

Jue Bai,[a] Weilian Fu,[b] and Jiangjie Chen [c,*]

The choice of furniture materials has a direct impact on thermal comfort, especially during prolonged contact. In this study, the COMSOL Multiphysics software was utilized to simulate the process of heat transfer from the human body, treated as a constant heat source, to the wood desktop material at a specific room temperature. By carefully adjusting various physical parameters, the specific effects of each factor on the change in contact temperature were thoroughly examined. Simultaneously, human body method experiments were conducted as a control to verify the simulation's accuracy against real-world conditions. Additionally, a systematic analysis was performed to explore the influence of various physical parameters, such as density, specific heat capacity, thermal conductivity, thickness, and decorative layer treatment, on temperature sensation. The primary objective was to address the existing challenge of achieving thermal comfort in wooden furniture design . The results suggest that the density, specific heat capacity, thermal conductivity, thickness, and room temperature of the wood tabletop material significantly affect the contact temperature. Applying coatings or veneers to the wooden tabletop can also influence the variation in contact temperature.

DOI: 10.15376/biores.20.4.10771-10794

Keywords: Wooden desktop; Finite elements; COMSOL multiphysics; Temperature sensing

Contact information: a: College of Fine Arts, Huaqiao University, Quanzhou, Fujian Province, China; b: College of Furnishings and Industrial Design, Nanjing Forestry University, Nanjing, Jiangsu Province, China; c: College of Fine Arts, Huaqiao University, Quanzhou, Fujian Province, China;
** Corresponding author: chenjiangjie@hqu.edu.cn*

INTRODUCTION

As the standard of living improves, people's demands for home environments are becoming more sophisticated. As a major category of furniture, tables and chairs account for a large proportion of the time spent working, studying, and living (Parry and Straker 2013). Prolonged contact with uncomfortable furniture causes cold, stuffy, and other unpleasant thermal sensations. Not only does this affect physical and psychological comfort at the time, but it can also cause health problems in the long term (Amin *et al*. 2015; Xiong *et al*. 2016; Ikei *et al*. 2017). Wood materials with lower thermal dissipation rates have been reported to achieve a higher surface temperature difference after 15 minutes of contact, providing a more comfortable tactile experience that is better suited for writing and daily use (Loredan *et al*. 2022). The Personalized Comfort System (PCS) is considered an effective alternative for delivering thermal comfort while reducing energy consumption (Rawal *et al*. 2020). Furniture panels can offer thermal comfort and have the potential to save energy.

Extensive research over many years has focused on the thermal sensations experienced by the human body when in contact with various materials. Such research has confirmed that the physical properties of materials significantly influence human thermal perception (Wang 2024). The local contact thermal comfort of furniture is the result of a combination of many factors, including material, thickness, furniture shape, ambient temperature and humidity, and contact pattern (Jumel *et al*. 2003). Surface finishes also impact thermal comfort upon contact with the human body. Even a veneer as thin as 1 millimeter, when applied to materials with high thermal conductivity, such as metal, can markedly change the perceived warmth or coolness of the substrate (Wang 2024). Consequently, the thermal comfort of furniture materials in direct contact with users is a significant factor influencing their physical and mental well-being. Material properties offer a more precise measurement of thermal comfort.

A combination of thermal comfort evaluation and instrumental measurements is typically employed to study the local contact thermal comfort of furniture. Subjective evaluation of thermal comfort and objective evaluation of thermal comfort are conducted through human experiments (Horikiri *et al*. 2015; Loredan *et al*. 2022). Subjective thermal comfort ratings involve the use of a thermal comfort questionnaire to directly assess people's thermal sensations and levels of comfort (Hasebe *et al*. 1995; Nastase *et al*. 2016). Objective thermal comfort evaluation is a method that reflects the thermal comfort of the human body by measuring changes in the physiological responses of the human body (Ferrarin and Ludwig 2000; Huizenga *et al*. 2004; Bulcao *et al*. 2016). Although human experimentation is the primary method for studying temperature sensation, that kind of approach is resource-intensive and time-consuming, and it introduces many uncertainties (Vlaović *et al*. 2012a). The experimental environment, individual differences of subjects, geography, and so on all affect the accuracy of human experiments. Consequently, many scientists are looking to use the simulated human body instead of the human body to conduct experiments (Cannon and Denhartog 2019). The study of thermal comfort through experimental equipment device simulation to replace the human body for experiments is a widely adopted simulation method (Vlaović *et al*. 2012b). The test device must replicate the temperature distribution of a real human body and be capable of providing continuous heat to maintain a constant surface temperature (Rugh *et al*. 2004). However, the costly and time-consuming trial-and-error experiments typical of traditional research significantly impede efficiency. This study systematically explored the thermal perception characteristics of wooden tabletops, integrating finite element simulation with human experimentation. Instead of merely serving as simple substitutes, these two methods are complementary and mutually validating. Finite element simulation offers a robust scientific foundation and powerful technical tools for the precise design and prediction of furniture material performance.

The proliferation and advancement of finite elements have significantly enhanced computer programs designed for simulating thermal environments (Neacsu *et al*. 2017; Ozcelik and Becerik-Gerber 2018). Utilizing simulation and modeling software to study the thermoacoustic properties of furniture materials can inspire innovative ideas for thermoacoustic research. The Finite Element Method (FEM) is an effective analytical tool for problems that traditional analytical methods cannot solve and for those involving complex boundary conditions and irregular structural shapes (Younes *et al*. 2010). This method has been extensively applied to simulate and address various problems in engineering mechanics (Yazid *et al*. 2009), thermal (Pérez-Aparicio *et al*. 2016), electromagnetism (Ramachandran *et al*. 2023), and other physical domains. The concept

behind the finite element method is to discretize the continuous solution domain of the research object into a finite number of interconnected elements (Schweitzer 2012). In recent years, finite element algorithms have undergone continuous development, and computer software based on these algorithms has seen increasing improvements. In this paper, COMSOL Multiphysics (hereinafter referred to as COMSOL) was applied. This is a finite-element-based numerical simulation software, which is widely recognized in fields such as physics (Trim *et al*. 2021), mechanics of machines (Acheli and Serhane 2015), electrical engineering (Andras *et al*. 2024), mechanics (Zhou *et al*. 2018), fluid flow (Zhou *et al*. 2019), and chemistry (Azad *et al*. 2016). The software's simulation capabilities allow for the flexible and precise coupling of mass, heat, and work transfer processes within a reaction (Gbenou *et al*. 2022). With its efficient computational resources and unique multi-field fully coupled analysis feature, COMSOL ensures the high accuracy of numerical simulations (Huang *et al*. 2021).

In this paper, COMSOL software was utilized to simulate the heat transfer process from a human body, considered a constant heat source, to a wooden desktop material at a specific room temperature. Finite element simulation is employed to simulate the change in contact temperature following the human body's interaction with the wooden desktop. Upon confirming the viability of the finite element simulation through the human body method, the study delves into the impact of various factors on the variation of contact temperature. It is important to highlight that human perception of warmth from furniture surfaces is significantly affected by the ambient temperature. This study primarily aimed to explore methods for reducing heat loss and improving the sensation of warmth by optimizing the thermophysical properties of wood materials in both normal and low-temperature conditions. The research meets the market's demand for high-quality, personalized furniture. In the long run, it is anticipated to propel the advancement of the furniture industry, enhance brand competitiveness, and promote employment and economic growth.

EXPERIMENTAL

Materials and Experimental Environment

The wood materials used in the experiment included medium-density fiberboard (MDF), single-layer structured particleboard (SPB), and poplar multilayer board (PLY), with dimensions of 500 mm × 500 mm × 20 mm (Czajkowski *et al*. 2016). The surface decorative materials consisted of acrylic varnish (AP) and decorative paper for wood-based panel finishes (DPW), each with a thickness of 1 mm. Prior to the commencement of the experiment, all samples were stored in the laboratory for more than 2 weeks. Fifteen adult males and 15 females each, who had no significant abnormalities in their perception of temperature and humidity, were selected as test subjects. They were between 20 and 30 years old and had regular daily activities such as eating and sleeping.

The laboratory was situated in Nanjing, Jiangsu Province, with plan dimensions of 5.2 m × 4.5 m × 3.0 m. Indoor air temperature and humidity were regulated by air conditioners and humidifiers, respectively. The experiments were carried out in a location that minimized unnecessary convective heat transfer from direct air conditioner airflow, which could lead to heat loss from the subjects' surfaces, causing thermoreceptor sensory imbalance. For general civil buildings, the indoor temperature of air conditioning is typically set to 25 °C in summer and 20 °C in winter, while the indoor temperature of

general civil buildings without air conditioning is generally between 30 and 35 °C in summer (Bai *et al*. 2022). Therefore, the three indoor temperatures of low (20 °C), medium (25 °C), and high (30 °C) were selected as the experimental ambient temperatures. Throughout the study, relative humidity (RH) was maintained at 50% ± 10% (Rawal *et al*. 2020).

Test Instruments

The thermal conductivity of the test materials was measured using a thermal conductivity meter, and the specific heat capacity was determined with a differential scanning calorimeter. The instrumental details are presented in Table 1.

Table 1. Main Test Instruments

Instrument Name	Model	Manufacturers	City	Country
Thermal conductivity meter	Hot Disk TPS2500S	Kegonas Instruments Co.	Shanghai	China
Differential scanning calorimeter	DSC 214	NETZSCH-Gerätebau GmbH	Shanghai	China
Multi-channel temperature logger	PT700-16	Shenzhen Toprie Electronics Co.	Shenzhen	China

Methods

Determination of test material properties

The densities of the wooden desktop material panels were all derived through weighing. The density of AP was tested by the Archimedean drainage method, volume of the dry coating by displacement. The mass of the coating, divided by its volume, yields its density. Initially, the dry coating was first made by applying wood varnish on PTFE sheets. Subsequently, the coating was peeled off and weighed. To measure its volume, the coating was secured with fine wire or silk mesh and subjected to Archimedes drainage method (Yu *et al*. 2021).

The thermal conductivity of the test materials was ascertained using a thermal conductivity meter, employing the transient plate heat source method. Additionally, the specific heat capacity of the materials was determined by a differential scanning calorimeter, utilizing the DSC sapphire method.

Human upper extremity temperature test

The test points for temperature measurement were selected from the tip of the middle finger (T_1), the palmaris major (T_2), and the lateral aspect of the forearm palm (T_3). These points had to be in close contact with the test material (Fig. 1). A temperature sensor on the test instrument was connected to the test points to check the contact temperature at each of the three points. Subjects wore standard clothing (thermal resistance 0.6 clo), with air largely at rest (wind speed 0.1 m/s), maintaining an air temperature equal to the mean radiant temperature (Sung *et al*. 2019) . After the start of the test, the subject's upper arm was in natural contact with the test material for 30 min, and the average contact temperature T_a was calculated using the formula as Eq. 1 (Jue and Huiyuan 2022):

$$T_a = 0.211T_1 + 0.211T_2 + 0.578T_3 \quad (1)$$

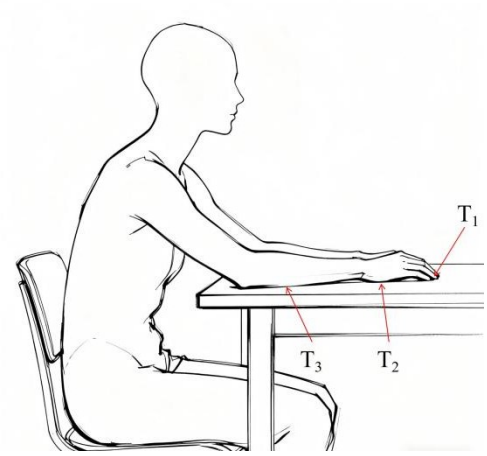

Fig. 1. Measurement of the subject's upper limb temperature

SIMULATION MODELING PROCESS

Defining Parameters

Before constructing the model, the initial step was to define the parameters for the wooden desktop material and the environmental conditions *via* the COMSOL parameter window. These parameters are the variables that need to be altered in the subsequent simulation, which can be set once through the definition window and do not require repeated adjustments within the model. The most important parameters relevant to all models are detailed in Table 2. T_m represents the core temperature of the human torso at rest, approximating the average temperature of the internal organs.

Table 2. COMCOL Definition Parameters

Name	Displayed Formula	Value	Description
L_q	1 (mm)	0.001 m	Thickness of surface decoration material
L_b	20 (mm)	0.02 m	Substrate material thickness
T_a	20 (°C)	20 °C	Indoor ambient temperature
T_m	38.5 (°C)	38.5 °C	Human core temperature

Note: The expression columns in the table are all variable

Plotting Analog Graphics

A 1:1 material model with dimensions of 500 mm × 500 mm × L (where L = L_a + L_b) was created using a 3D simulation physical model generated by COMSOL Multiphysics field software, as depicted in Fig. 2. The human upper extremity was simplified to a rectangular body with rounded corners of 60 mm × 30 mm × 200 mm, serving as a constant temperature heat source for heat dissipation.

When drawing the wood desktop material, the wood desktop material was divided into two layers, L_a (device material) and L_b (substrate material), through the layering operation in COMSOL geometry generation. After the geometric modeling, a boundary probe was defined at the contact interface between the thermostatic heat source of the human upper extremity and the wood desktop material to find the average contact temperature at the contact surface, T_s, using a fourth-order integration.

The Environment property was selected from the common properties, with the ambient temperature set to L_a and the ambient humidity was set to 50%. The wind speed in an indoor environment is typically low, and therefore, it was directly ignored.

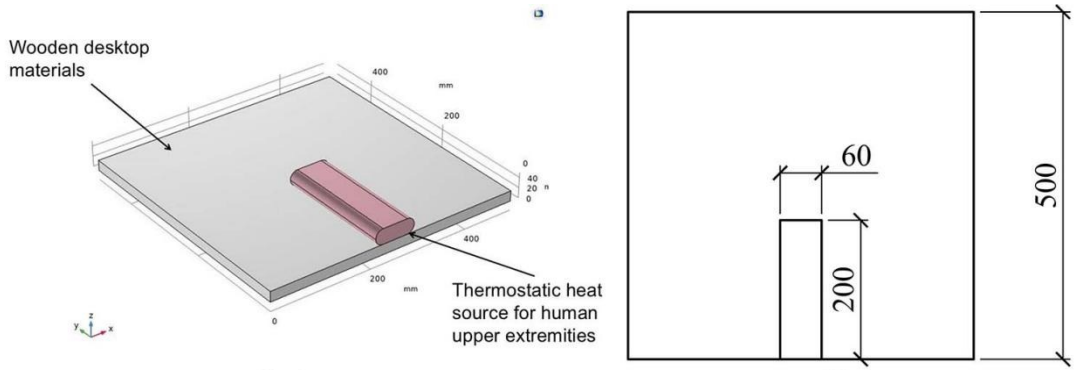

Fig. 2. Dimensions of the 3D model

Input Material Parameters

When utilizing the Solid Heat Transfer Module to simulate heat transfer in COMSOL, it is necessary to input the physical property parameters of various materials, as displayed in Table 3. To add a new material, the user locates the Material option in the menu bar and defines the properties of each material in the designated section.

Table 3. Nature of the Test Material

Number	Name	Density (ρ) kg•m^{-3}	Specific Heat Capacity (C) J•(kg•K)$^{-1}$	Thermal Conductivity (λ) W•(m•K)$^{-1}$
1	MDF	700.76	1492	0.2
2	SPB	59068	1662	0.1968
3	PLY	565.62	1690	0.189
4	AP	1088.5	1645	0.058
5	DPW	940	2030	0.12

Setting Boundary Conditions

Before establishing the boundary conditions, it is essential to analyze the model's heat transfer process and the underlying assumptions:

(1) The wooden tabletop material itself has no internal heat source. The surface temperature of the contact material varies with the temperature of the upper extremity heat source. The material's length and width are significantly larger than its thickness, allowing it to be considered as a semi-infinite flat plate undergoing a solid thermal conductivity process.

(2) The heat transfer process in the ambient temperature remains essentially constant; the thermal conductivity of the material does not change with time or temperature. The impact of water vapor and humidity on the heat transfer process is negligible.

(3) Heat transfer primarily occurs through three different thermal modes: conduction, radiation, and convection. This paper focuses solely on the heat transfer *via* thermal conductivity, and the other modes are not taken into account.

Based on the analysis of boundary conditions, the COMSOL Solid Heat Transfer module was selected for simulation:

(1) The simulation of the human upper limb part of the human body includes a fixed initial temperature, T_m, while the wooden desktop material has an initial value of T_a.

(2) External natural convective heat flow is set for the top and bottom sides of the wooden material, and other parts are set to standard thermal insulation.

(3) A boundary heat source is set at the contact surface between the human body's constant temperature heat source and the wooden desktop material, with a generalized source Q = 30 W/m^2.

(4) A thin layer is set on the part of the finish material, and the layer type is defined as a thermally thin approximation. The physical properties of the heat transfer are the same as those of the finish material set in the material properties.

Selecting the Grid

Finite element meshing significantly influences the accuracy of the results and the computational size within model (Li *et al*. 2006). In this model, computational cells, such as thin layers, necessitate more precise calculations. Therefore, a smaller mesh subdivision is required in the thin layer part compared to other areas. A refined grid is employed in the thin layer section, while a regular grid is utilized in the remaining parts.

Computational Simulation Results

The solid heat transfer results were calculated using the transient solver over a period of 1500 s. The boundary probe value in the calculation results represents the temperature change from the finite element simulation.

Finite Element Simulation Verification

After conducting the COMSOL simulation of the wood desktop material, the temperature change curves produced by the finite element simulation were compared with the average contact temperature curves obtained through the human body method, and the simulation errors were analyzed. Bootstrap confidence intervals were constructed for the simulation predictions based on human experimental data. This method calculates 95% confidence intervals for simulation errors using resampling techniques, offering a more intuitive representation of the uncertainty and precision of simulation predictions. It is independent of strict distribution assumptions. Statistical Product and Service Solutions (SPSS) was utilized to conduct correlation analysis for significance, assessing the impact of categorical variables, such as different materials (MDF, PB, and PLY), thicknesses, and decorative treatments, on the final temperature (at 1500 seconds). Subsequently, factor analysis was employed to identify the most influential factors (Du *et al*. 2023)

RESULTS AND DISCUSSION

COMSOL Finite Element Simulation Feasibility Analysis

The contact microenvironment of the wooden desktop was simulated using COMSOL. The simulation at 1500 s is depicted in Fig. 3, taking the contact with MDF at

20 °C as an example. Heat dissipates from the upper limb heat source, traveling from top to bottom and spreading to the surrounding area. Heat dissipation around the perimeter is insufficient to reach the material boundary, but the normal direction has a significant impact, mirroring real-world conditions. The model's transient solution process involves iterative calculations that approach the true value. When the calculation error converges after the final iteration, the value is infinitely close to the true value. The final convergence value of the model for contact with the MDF at 20 °C is less than 0.01, indicating that the calculated value is close to the true value as it converges during iteration.

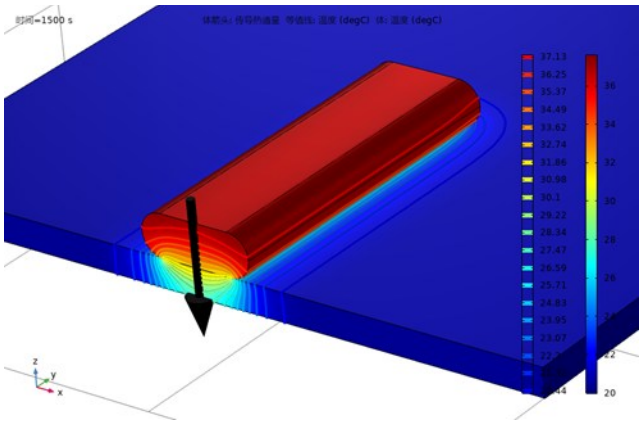

Fig. 3. COMSOL simulation of heat transfer

Simulation Verification of Undecorated Wooden Tabletop Materials

After conducting a COMSOL finite element simulation on the wooden desktop material, the contact temperature was recorded every 6 s, resulting in a temperature change curve T_s over a period of 1500 s. Simultaneously, the temperature change curve T_a of human contact with the wooden desktop material was also documented every 6 s throughout the same 1500-second duration. The comparison results between the simulated value T_s and the experimental value T_a are depicted in Figs. 4, 5, and 6. The resting temperature of the human torso is typically 36.8 °C, with skin temperature dropping below its resting average (33.7 °C), particularly in distal body parts such as hands and feet (Laouadi 2024). T_a reflects the body's temperature response when exposed to cold conditions and in contact with materials. The figures illustrate the 95% confidence interval derived from the sampling of test data, indicating that the simulated data falls within this interval, which signifies an excellent fit (Julious *et al*. 2007). The temperature-time curves for the human body method test values and the finite element simulation values exhibit similar trends. Regarding simulation error, the initial error is relatively large but diminishes over time, meaning the tested and simulated values converge. At lower room temperatures (20 °C), the discrepancy between the temperature profiles of the finite element simulation and the experimental data is more pronounced. However, as the room temperature rises, the simulated curve becomes more aligned with the actual curve.

The average error and the percentage of this average error between the human upper extremity temperature test values and the finite element simulation values are presented in Table 4. The average temperature error between the measured and simulated results is within 0.3 °C. In terms of human temperature perception, a temperature difference of 0.3 °C is unlikely to cause a perceptible change. The average error percentage between the subjects' measured results and the simulation is within 0.7%, suggesting that the COMSOL

simulation software can accurately replicate the micro-interface temperature changes of the human upper limb when in contact with a single-layer wooden desktop.

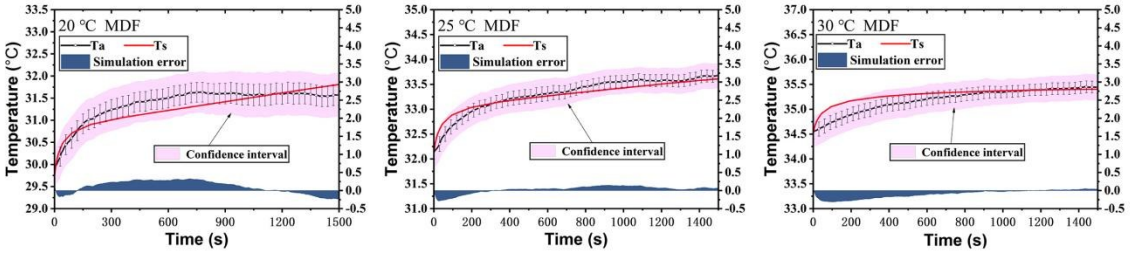

Fig. 4. Comparison of the average temperature variation of MDF under different room temperature environment by finite element simulation and human upper extremity temperature test

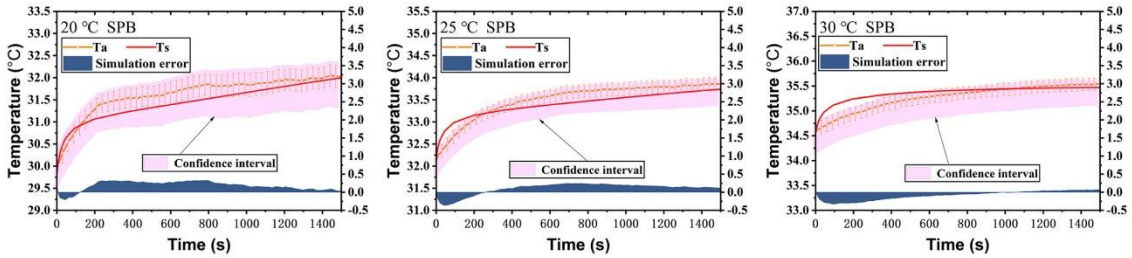

Fig. 5. Comparison of the average temperature variation of SPB under different room temperature environments by finite element simulation and human upper extremity temperature test

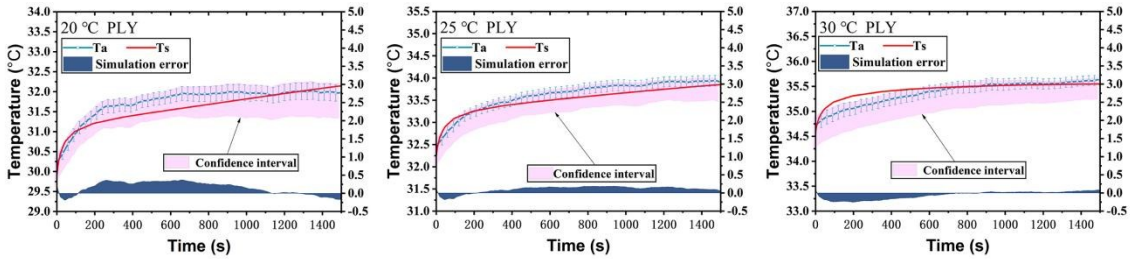

Fig. 6. Comparison of the average temperature variation of PLY under different room temperature environments by finite element simulation and human upper extremity temperature test

Table 4. Finite Element Simulation Error Situation

Materials	20 °C		25 °C		30 °C	
	Average Error	Mean Error as a Percentage (%)	Average Error	Mean Error as a Percentage (%)	Average Error	Mean Error as a Percentage (%)
MDF	0.177	0.563	0.086	0.258	0.108	0.308
SPB	0.201	0.636	0.175	0.522	0.113	0.322
PLY	0.194	0.612	0.128	0.379	0.091	0.258

Note: The average error is the average of the absolute value of the error; the average error as a percentage is the average of the absolute value of the error as a proportion of the test value

Finite element simulations were conducted on a single layer of MDF with varying thicknesses of wood desktop material at a room temperature of 25 °C. The comparison between the finite element simulation results and the test values from human upper extremity temperature tests is shown in Fig. 7. The temperature-time curves for different thicknesses of MDF boards exhibit similar trends. The curves of the simulated values and the test values align well, indicating that the temperature changes are more stable and the error trends were comparable.

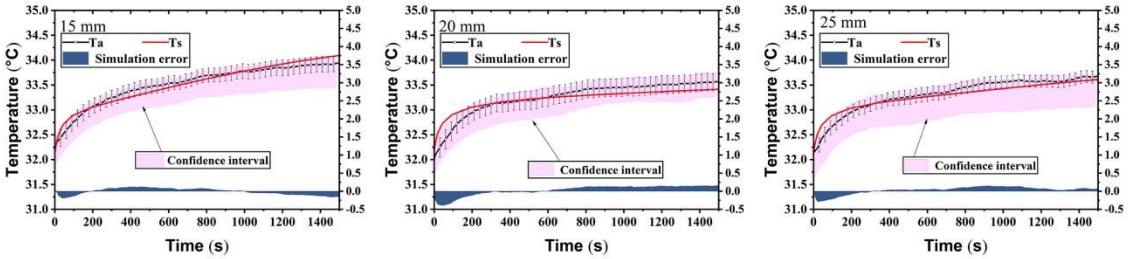

Fig. 7. Comparison of average temperature variation between finite element simulation and human body method test for different thickness of MDF

Table 5 displays the average error and the percentage of this error between the values obtained from human body method tests and the finite element simulations for various thicknesses of MDF. The average temperature error between the measured and simulated outcomes was limited to 0.2 °C. A temperature variance of 0.2 °C is typically imperceptible to the human body. Furthermore, the average error percentage between the subjects' measurement outcomes and the simulation remains below 0.4%, a small margin that suggests finite element simulations can accurately mimic the human body's interaction with wooden desktop materials of varying thicknesses.

Table 5. Finite Element Simulation Error Situation

Thicknesses (mm)	Average Error	Mean Error as a Percentage (%)
15	0.078	0.233
20	0.086	0.258
25	0.114	0.343

Note: The average error is the average of the absolute value of the error; the average error as a percentage is the average of the absolute value of the error as a proportion of the test value

Simulation Validation of Wood Desktop Materials After Surface Decoration

After conducting a finite element simulation of the MDF wood desktop material post-surface decoration, the simulated temperature value T_s is presented in Fig. 8, alongside the temperature change T_a derived from the medium human body method test. The temperature-time curves of both the experimental and simulated values exhibit a similar trend, with a small difference between them and a good curve fit.

The average error and percentage of the average error between the human body method test values and the finite element simulation values for the wood tabletop material after surface decoration are shown in Table 6. The average error in temperature between the measurement results and the simulation results was within 0.2 °C. The average error percentage between the subjects' measurements and simulations was within 0.5%, indicating that the device developed in this study was able to accurately simulate the

contact temperature between the forearm and the surface-decorated wooden desktop material.

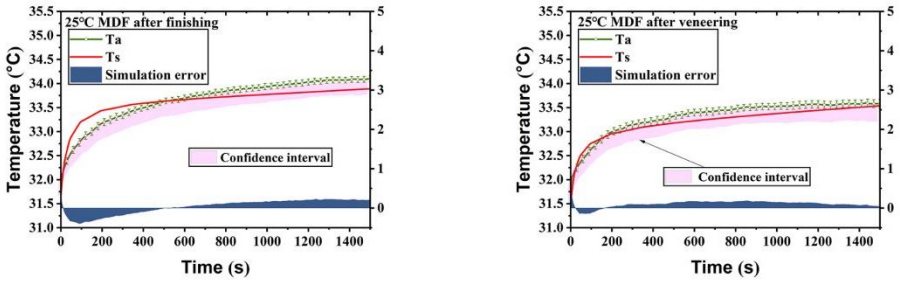

Fig. 8. Comparison of average temperature change between MDF finite element simulation and anthropometry test after surface decoration

Table 6. Finite Element Simulation Error Situation

Surface Decoration Method	Average error	Mean Error as a Percentage (%)
Paint	0.165	0.491
Veneer	0.119	0.358

Note: The average error is the average of the absolute value of the error; the average error as a percentage is the average of the absolute value of the error as a proportion of the test value

Factors Affecting the Contact Temperature of Wooden Table Tops

Methods of analysis

According to the classical solid-state heat transfer theory, the heat transfer situation is influenced by several factors: the material density ρ (kg/m^3), the material heat capacity C_p (J/(kg·°C)), the material thermal conductivity k (W/(m·°C)), the material thickness δ (mm), the heat source term Q (W/m^3), and the temperature gradient ∇T. In addition, the heat transfer properties of multilayer materials necessitate consideration of both the number of layers and the individual material properties. To investigate the impact of each factor on the contact temperature, a one-factor-at-a-time analysis is employed, where all other factors are held constant while one is varied, allowing for the examination of various material combinations in heat transfer simulations. Temperature fluctuations in the contact microenvironment under different conditions were analyzed using a finite element simulation of heat transfer from a wooden desktop. SPSS correlation analysis indicated that at 1500 seconds, the contact temperature was significantly correlated with the influencing factors, with all significance tests yielding p-values less than 0.05. Density, specific heat capacity, thermal conductivity, and thickness all exhibited negative correlations with contact temperature, with correlation coefficients $r < 0$, whereas room temperature demonstrated a positive correlation with contact temperature at 1500 seconds, with a correlation coefficient $r > 0$.

Heat transfer analysis of single-layer wood materials

(1) Analysis of wood tabletop materials with different densities

The ambient temperature was fixed at 25 °C, the material thickness was 20 mm, the heat capacity was 1492 J/(kg·°C), and the thermal conductivity was 0.2 W/(m·°C). The variable in question was the density, with gradients of 400, 500, 600, 700, 800 and 900 kg/m^3. The variation of the average surface temperature after simulation by COMSOL is depicted in Fig. 9(A). The temperature variation is inversely proportional to the density, *i.e.*, a higher density correlates with a lower temperature and a flatter temperature trend.

A comparison of the polar difference between the highest and lowest temperatures is illustrated in Fig. 9(B). The extreme deviation diminishes with increasing density, suggesting that a higher density results in a lower rate of temperature change.

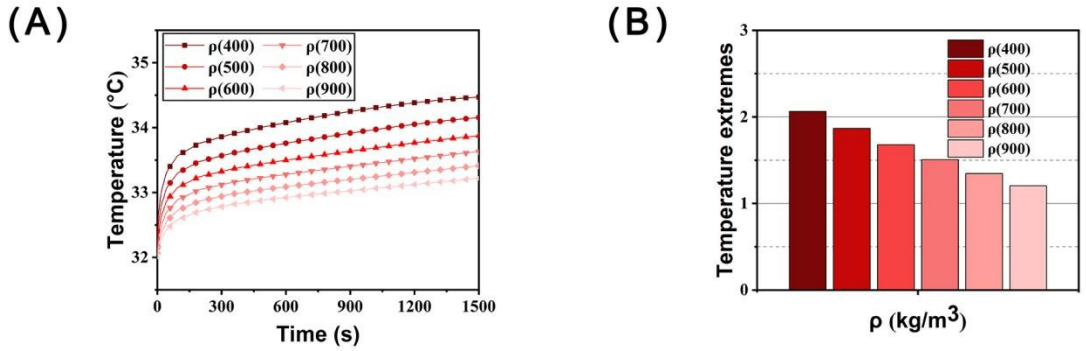

Fig. 9. Finite element simulation of materials with different densities: (A) Temperature change; (B) temperature extremes

(2) Analysis of wood tabletop materials with different heat capacities

The ambient temperature was fixed at 25 °C. The material was 20 mm thick, with a density of 700.8 kg/m³ and a thermal conductivity of 0.2 W/(m·°C). The variable in question was the specific heat capacity, which exhibited a gradient of 1,000, 1,200, 1,400, 1,600, 1,800, and 2,000 J/(kg·°C). Following simulation with COMSOL, Fig. 10(A) shows the variation of the average surface temperature. The temperature variation is inversely proportional to the heat capacity; that is, a higher heat capacity corresponds to a lower temperature. Despite this, the overall temperature trend remains consistent. Figure 10(B) depicts the difference between the highest and lowest temperatures. As the heat capacity increases, the extreme temperature difference diminishes. This indicates that a higher heat capacity results in a smaller the temperature change rate. However, when compared to density, the rate of change in the extreme temperature difference due to heat capacity is relatively small, suggesting that heat capacity has a minor influence on the temperature trend.

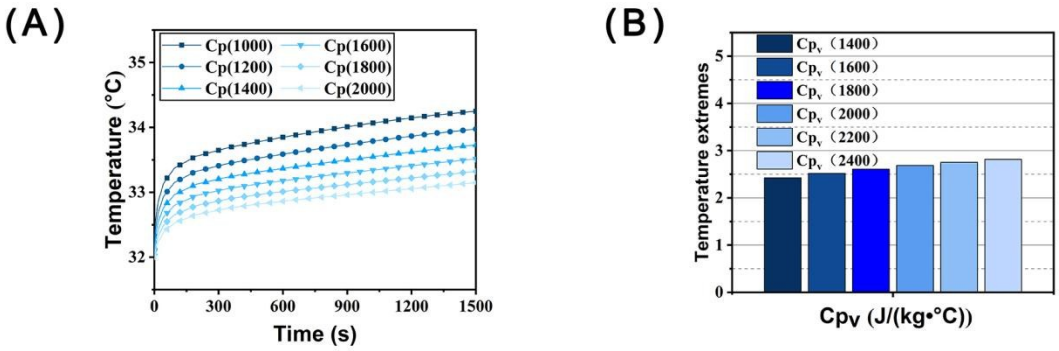

Fig. 10. Finite element simulation of materials with different heat capacities: (A) Temperature change; (B) temperature extremes

(3) Analysis of wood tabletop materials with different thermal conductivity

The ambient temperature was set at 25 °C. The material was 20 mm thick, with a density of 700.8 kg/m³, and a heat capacity of 1492 J/(kg·°C). The thermal conductivity varied with gradients of 0.05, 0.1, 0.15, 0.2, 0.25, and 0.3 W/(m·°C). After simulating with

COMSOL, Fig. 11(A) illustrates the average surface temperature change, which is inversely proportional to thermal conductivity; in other words, higher thermal conductivity corresponds to lower temperatures and a smoother the temperature change trend. As depicted in Fig. 11(B), comparing the extreme difference between the highest and lowest temperatures, the difference diminishes with increasing thermal conductivity. That is, higher thermal conductivity results in a smaller the temperature change rate. At lower thermal conductivity values, the extreme difference is larger. However, as thermal conductivity increases, the difference between these extremes narrows. This means that the thermal conductivity has a more significant impact on temperature change in cases of lower conductivity.

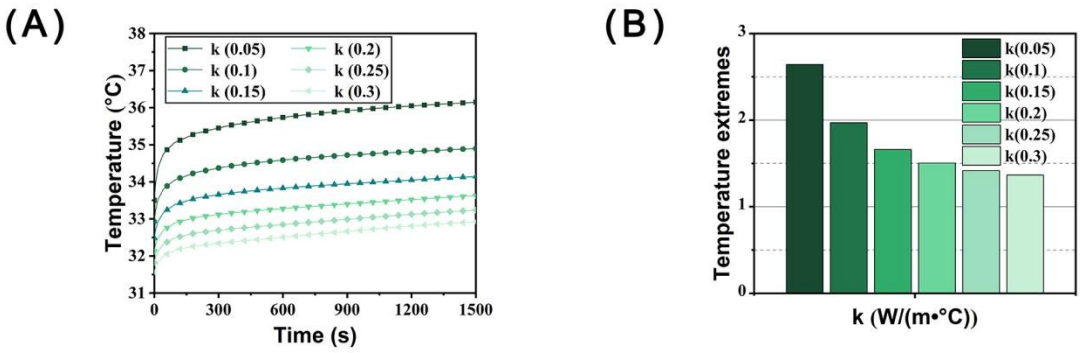

Fig. 11. Finite element simulation of materials with different thermal conductivity: (A) Temperature change; (B) temperature extremes

(4) Analysis of wood tabletop materials with different thicknesses

The ambient temperature was fixed at 25 °C, the density was 700.8 kg/m³, the heat capacity was 1,492 J/(kg·°C), and the thermal conductivity was 0.2 W/(m·°C). The variable under examination was the thickness of the material, which ranged from 20 to 45 mm in increments of 5 mm.

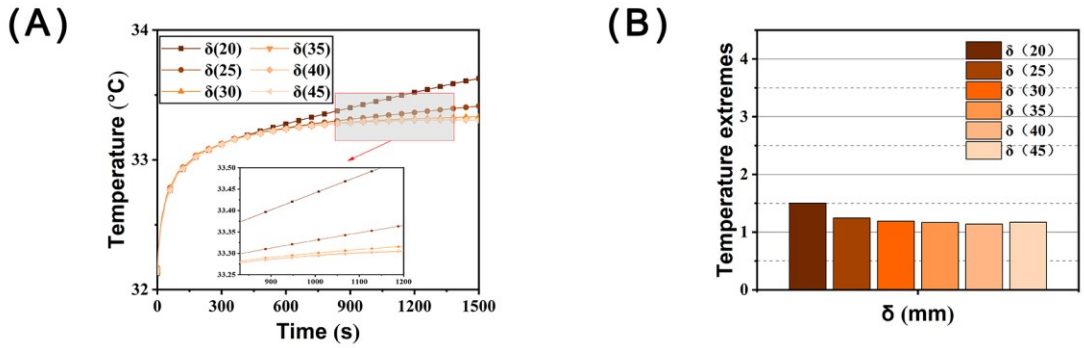

Fig. 12. Finite element simulation of materials with different thicknesses: (A) Temperature change; (B) temperature extremes

Following simulations conducted with COMSOL, Fig. 12(A) illustrates that the average surface temperature change is inversely proportional to the material's thickness. In other words, as the material becomes thicker, the surface temperature decreases, and the rate of temperature change becomes more gradual. As shown in Fig. 12(B), when comparing the extreme difference between the highest and lowest temperatures, it is

evident that this difference diminishes with increasing thickness. This indicates that a thicker material results in a smaller the temperature change rate. Conversely, at thinner sections, the extreme temperature difference is more pronounced, suggesting that increasing the material's thickness leads to a more gentle stable temperature variation.

(5) Analysis of wood tabletop materials with different indoor temperatures

In this study, a fixed heat source is employed, which allows for the control of the room temperature (T_a) and, consequently, the temperature gradient (∇T). The material under investigation had a thickness of 20 mm, a density of 700.76 kg/m³, a heat capacity of 1492 J/(kg·°C), and a thermal conductivity of 0.2 W/(m·°C). The variable in the experiment was the room temperature (T_a), which was set to various gradients: 20, 22, 24, 26, 28, and 30 °C. The material's temperature was measured under exposure to a gradient of 0.2 W/(m·°C). Simulations conducted using COMSOL revealed that the average surface temperature, as depicted in Fig. 13(A) , changes proportionally with the room temperature. In other words, as the room temperature rises, so does the surface temperature, resulting in a smoother the temperature trend. As shown in Fig. 13(B), the extreme difference between the highest and lowest temperatures diminishes with increasing room temperature. This indicates that at higher room temperature, the rate of temperature change is smaller. Conversely, at lower room temperatures, the extreme difference is more pronounced, suggesting that the rate of temperature change is more gradual and stable in warmer environments.

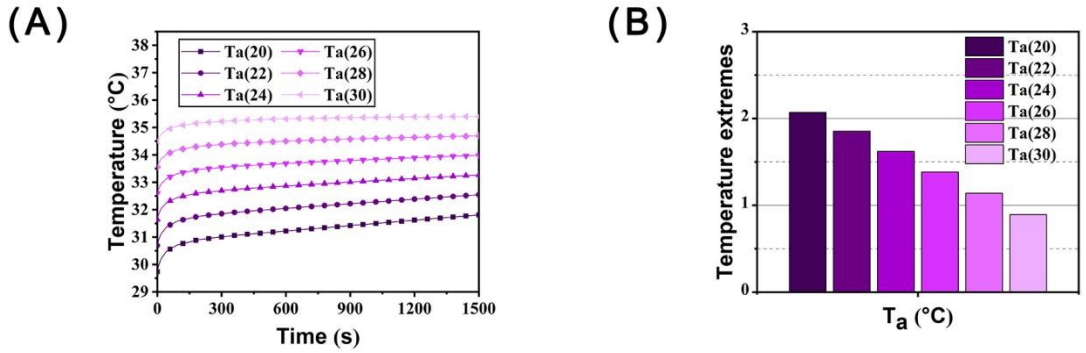

Fig. 13. Finite element simulation of materials with different indoor temperatures: (A) Temperature change; (B) temperature extremes

Heat transfer analysis of coated wood materials

The SPSS variable correlation analysis indicated that all significance tests (Sig.) for the correlation between contact temperature at 1500 seconds and coating factors yielded p-values less than 0.05, signifying statistically significant correlations. The correlation coefficients (r) for coating density, specific heat capacity, and thermal conductivity with contact temperature were all below zero, suggesting negative correlations. In contrast, the correlation coefficient (r) for coating thickness with contact temperature at 1500 seconds was above zero, indicating a positive correlation.

(1) Wood tabletop materials with different thicknesses of finishes

The ambient temperature and substrate properties were set based on the values presented in Table 7. The density of the coating was 1,088.5 kg/m³, its heat capacity was 545 J/(kg·°C), and its thermal conductivity was 0.05 W/(m·°C). The variable in question was the coating thickness (δ_c), which had gradients of 0, 0.2, 0.4, 0.6, 0.8, and 1 mm.

Table 7. Ambient Temperature and Substrate Properties

Nature	Ambient Temperature (°C)	Density (kg/m³)	Heat Capacity J/(kg • °C)	Thermal Conductivity W/(m • °C)	Heat Capacity J/(kg • °C)	Thickness (mm)
Numerical values	25	700.76	1,492	0.2	1,492	20

After simulating with COMSOL, Fig. 14(A) shows the variation in the average surface temperature, indicating that as the coating thickness increases, the heat transfer properties tend to align with those of the coating material. The coating exhibits low heat capacity and thermal conductivity. During the heat transfer process, the reduced ability to transfer heat results in an elevated contact temperature. Thus, as the coating thickness increases, so does the contact temperature, suggesting a proportional relationship between thickness and contact temperature. Figure 14(B) depicts the significant disparity between the maximum and minimum temperatures before and after the application of the coating. Prior to the coating, the temperature extremes were minimal, but post-coating, the temperature extremes have widened, suggesting that the surface coating alters the rate of temperature change. As the coating thickness increases, the temperature difference diminishes, implying that a thicker coating leads to a reduced rate of temperature change and a more stable the temperature profile. However, the overall temperature extremes do not vary substantially. In essence, while the coating thickness influences the rate of temperature change, the effect is not pronounced.

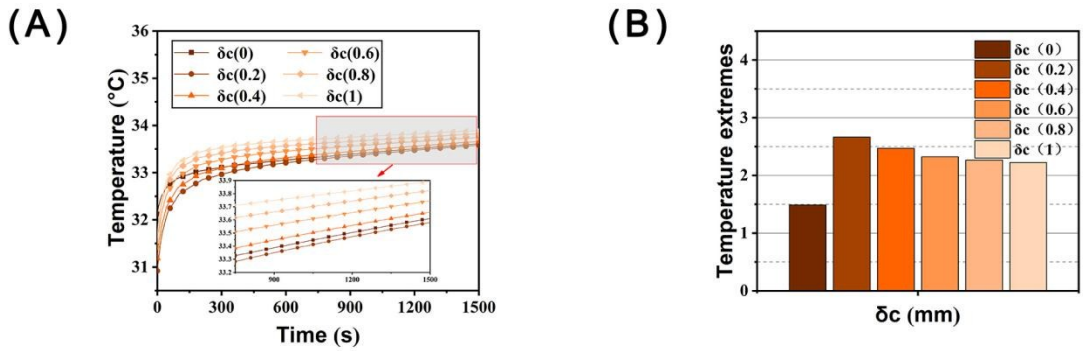

Fig. 14. Finite element simulation of materials with different thicknesses of finishes: (A) Temperature change; (B) temperature extremes

(2) Wooden desktop materials with different finishing densities

The ambient temperature and substrate properties were set according to the values presented in Table 7. The coating thickness was 0.2 mm, the heat capacity was 545 J/(kg · °C), and the thermal conductivity was 0.05 W/(m · °C). The variable under examination was the density of the coating (ρ_c), defined as the density of the dry film of the coating. The gradient was divided into six levels: 900, 1000, 1100, 1200, 1300, and 1400 kg/m³.

Following the COMSOL simulation, Fig. 15(A) shows the average temperature change of the surface. It was observed that the density of the paint film has a minor impact on the overall temperature range. Overall, the contact temperature decreases slightly as the density of the paint film increases; however, this difference is minimal. As depicted in Fig. 15(B), the variation in the extreme temperature differences among different paint film

densities is small, indicating that the effect of paint film density on contact temperature change is relatively insignificant.

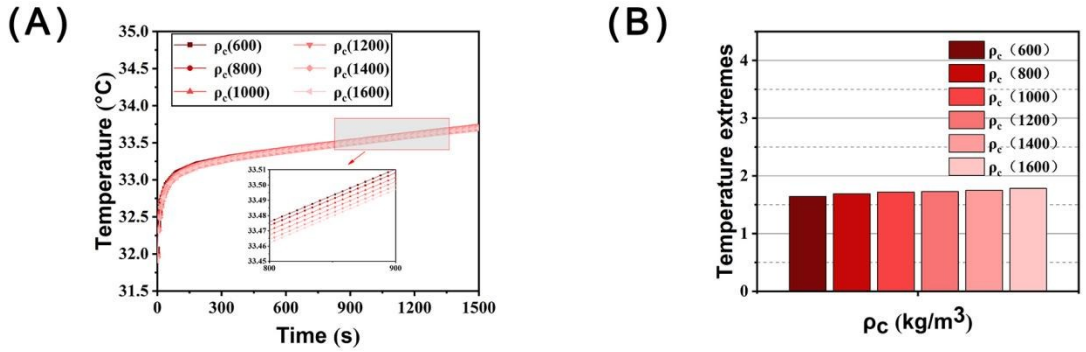

Fig. 15. Finite element simulation of materials with different finishing densities: (A) Temperature change; (B) temperature extremes

(3) Wooden desktop materials coated with different specific heat capacities

The ambient temperature and substrate properties were set based on the values presented in Table 7. The coating's thickness measured 0.2 mm, its density was 1,088.5 kg/m³, its thermal conductivity was 0.05 W/(m·°C), and the variable under examination was the coating's heat capacity (Cp_c), which exhibited gradients of 600, 800, 1,000, 1,200, 1,400, and 1,600 J/(kg·°C).

After the COMSOL simulation, Fig. 16(A) shows the variation in average surface temperature. It becomes evident that increasing the heat capacity of the coating has a negligible effect on the overall temperature range.

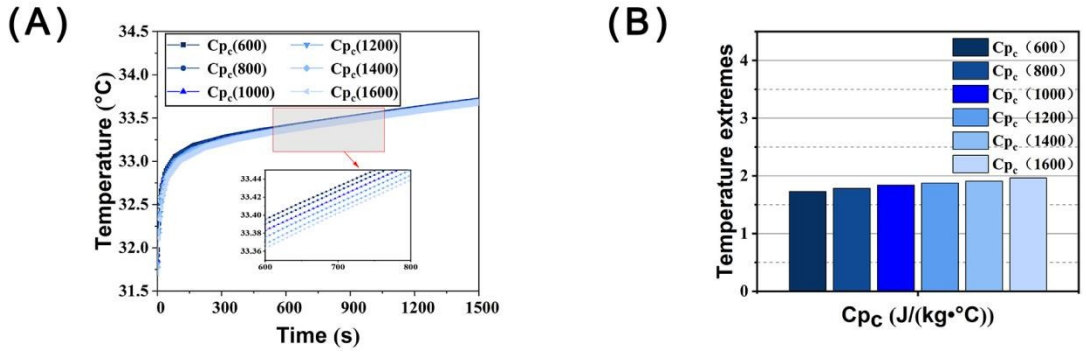

Fig. 16. Finite element simulation of materials coated with different specific heat capacities: (A) Temperature change; (B) temperature extremes

Overall, the contact temperature decreases as the paint film density increases, although the difference is slight. As depicted in Fig. 16(B), the difference in contact temperature among paint films with varying heat capacities is minimal, indicating that the density of the paint film has a relatively small effect on contact temperature change.

(4) Wooden desktop materials coated with different thermal conductivity

The ambient temperature and substrate properties were set based on the values shown in Table 7. The coating thickness was 0.2 mm, the density was 1088.5 kg/m³, the

heat capacity was 545 J/(kg·°C), and the thermal conductivity (k_c) was the variable with gradients of 0.02, 0.04, 0.06, 0.08, 0.1, and 0.12 W/(m·°C).

The average surface temperature change is depicted in Fig. 17(A). The temperature change is inversely proportional to the thermal conductivity of the paint film, *i.e.*, higher thermal conductivity corresponds to lower temperature and a flatter temperature trend. Comparing the extreme difference between the highest and lowest temperature, as shown in Fig. 17(B), the extreme difference diminishes with increasing thermal conductivity. This means that a higher coefficient of thermal conductivity results in a lower rate of temperature change. In cases with a smaller coefficient of thermal conductivity, the extreme difference is larger. However, as the coefficient of conductivity increases, the difference between the highest and lowest temperatures decreases, indicating that a smaller coefficient of thermal conductivity leads to a relatively greater influence of the temperature change.

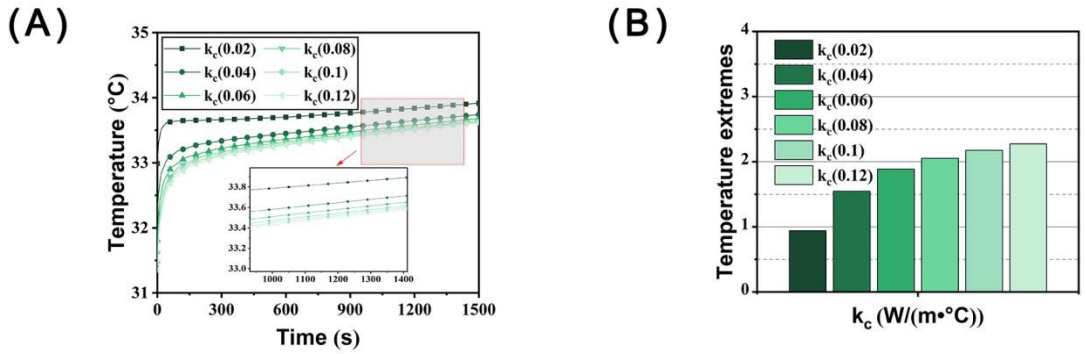

Fig. 17. Finite element simulation of materials coated different thermal conductivity: (A) Temperature change; (B) temperature extremes

Heat transfer analysis of wood desktop material veneer

The SPSS variable correlation analysis revealed that all significance tests (Sig.) for the correlation between contact temperature at 1500 °C and wood desktop material veneer properties yielded p-values of less than 0.05, indicating statistically significant correlations. The correlation coefficients (r) between contact temperature and veneer material properties (density, specific heat capacity, thermal conductivity, and thickness) were all less than zero, indicating negative correlations.

(1) Wooden tabletop materials with different veneer thicknesses

The ambient temperature and substrate properties were set according to the values shown in Table 7. The veneer density was 940 kg/m^3, the heat capacity was 2030 J/(kg ·°C), and the thermal conductivity was 0.12 W/(m·°C). The variable in question is the thickness of the veneer (δ_v), which was divided into gradients of 0, 0.2, 0.4, 0.6, 0.8, and 1 mm.

Figure 18(a) shows the average surface temperature changes after the COMSOL simulation. As the veneer thickness increases, the nature of heat transfer changes. The heat transfer becomes more similar to that of the veneer. Given that the veneer's density and heat capacity are relatively large, heat transfer occurs relatively quickly. Therefore, as the veneer thickness increases, the contact temperature decreases; the two are inversely proportional. However, overall, increasing the veneer's thickness has a small effect on the contact temperature; the temperatures between each gradient are relatively close. As shown

in Fig. 18(B), comparing the extreme difference between the highest and lowest temperatures, the temperature difference is small before the veneer is applied. After the veneer is applied, the temperature difference increases, and the surface finish affects the temperature rate. As the veneer's thickness increases, the extreme difference gradually decreases. This indicates that the thicker the veneer, the smaller the temperature change rate and the more stable the temperature curve. However, the extreme difference in temperature does not change significantly. In other words, the thickness of the veneer affects the rate of temperature change, but the effect is not pronounced.

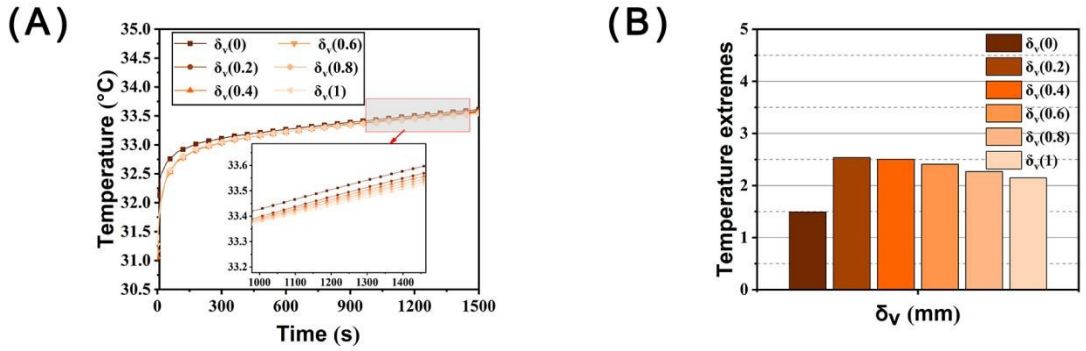

Fig. 18. Finite element simulation of veneer materials with different thicknesses: (A) Temperature change; (B) temperature extremes

(2) Wooden tabletop materials with different density veneers

The ambient temperature and substrate properties were set according to the values indicated in Table 7. The veneer's thickness was 1 mm, its heat capacity was 2030 J/(kg·°C), and its thermal conductivity was 0.12 W/(m·°C). The variable under examination was the veneer's density (ρ_v), with gradients of 500, 600, 700, 800, 900, and 1000 kg/m³.

After simulating the process using COMSOL, the average surface temperature changes are depicted in Fig. 19(A). During the process of increasing the veneer density, it was observed that the veneer density has a negligible effect on the overall temperature range. The general trend indicates that the contact temperature decreases as the veneer density increases; however, this difference is slight. As density increases, the polar variation of temperature change gradually intensifies, as shown in Fig. 19(B).

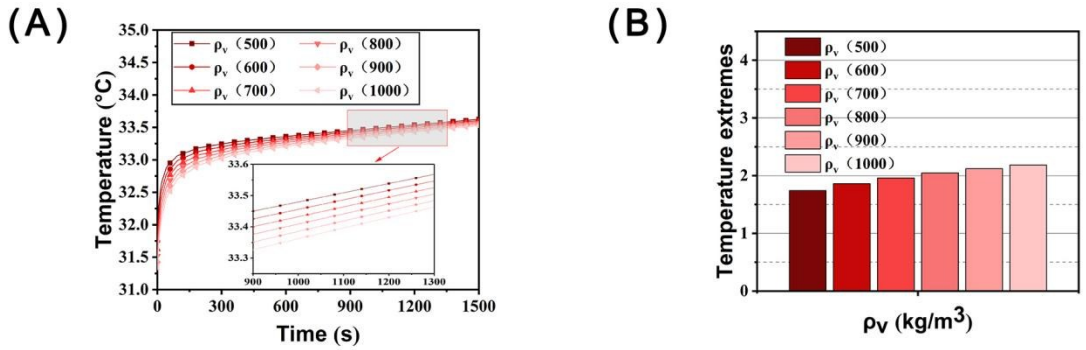

Fig. 19. Finite element simulation of veneer materials with different densities: (A) Temperature change; (B) temperature extremes

(3) Wooden tabletop materials with different specific heat capacity veneers

The ambient temperature and substrate properties are set according to the values indicated in Table 7. The veneer has a thickness of 1 mm, a density of 940 kg/m³, a thermal conductivity of 0.12 W/(m·°C), and a variable specific heat capacity (Cp_v). The gradient is divided into increments of 1400, 1600, 1800, 2000, 2200, and 2400 J/(kg·°C).

Figure 20(A) illustrates the variation of the average surface temperature following simulation with COMSOL. As the heat capacity of the veneer increases, the overall temperature range experiences a slight change. Overall, with an increase in the heat capacity of the veneer, the contact temperature decreases, although the difference is minimal. As shown in Fig. 20(B), an increase in density results in a gradual rise in the polar variation of the temperature change and an acceleration in the rate of temperature change; however, the difference is minor.

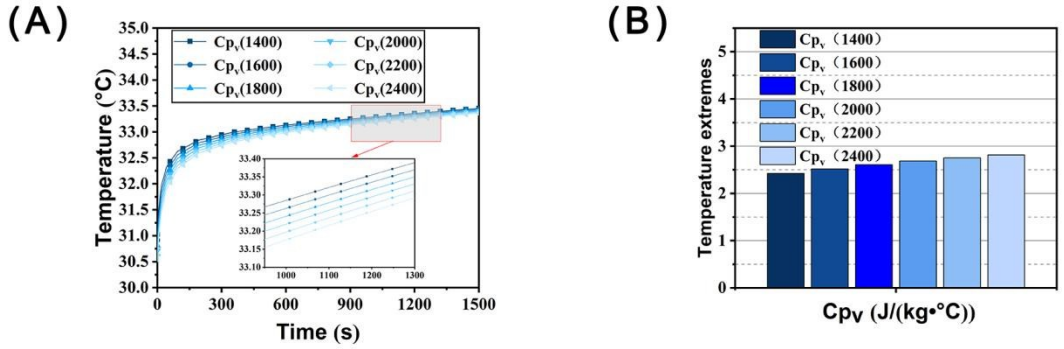

Fig. 20. Finite element simulation of veneer materials with different specific heat capacities: (A) Temperature change; (B) temperature extremes

(4) Wooden tabletop materials with different thermal conductivity veneers

The ambient temperature and substrate properties are set according to the values shown in Table 7. The veneer has a thickness of 1 mm, a density of 940 kg/m³, a heat capacity of 2030 J/(kg·°C), and a variable thermal conductivity (k_v), which is divided into 0.06, 0.08, 0.1, 0.12, 0.14, and 0.16 W/(m·°C).

The COMSOL simulation illustrates the average surface temperature change post-simulation in Fig. 21(A). The temperature change and thermal conductivity of the veneer are inversely proportional; in other words, the higher the thermal conductivity, the lower the temperature and the more gradual the temperature change trend. The impact is more pronounced. Figure 21(B) depicts the difference between the highest and lowest temperatures. As thermal conductivity increases, so does the disparity difference between the highest and lowest temperatures. In other words, the greater the thermal conductivity coefficient, the greater the impact on the temperature change.

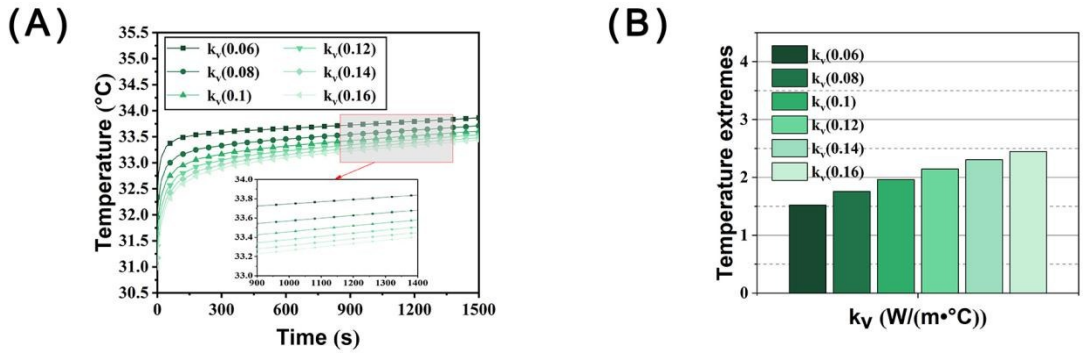

Fig. 21. Finite element simulation of veneer materials with different thermal conductivity: (A) Temperature change; (B) temperature extremes

CONCLUSIONS

1. The finite element method, when utilized with COMSOL software, offers a robust tool for simulating the thermal properties of wooden desktop materials. When this method is combined with and validated by targeted human experiments, it can substantially decrease the time and material usage typically required for extensive experimental campaigns, all while preserving a high level of accuracy and reliability.
2. A comparison of the simulated data with data from the human experiments reveals that the COMSOL simulation results align well with the experimental data, and the simulation error is within an acceptable range (within 0.2 °C). This indicates that the method accurately reflects microenvironmental temperature changes when the human body is in contact with a wooden desktop.
3. COMSOL simulated these changes to investigate how the density, specific heat capacity, thermal conductivity, thickness, and room temperature of wooden desktop materials affect contact temperature. For undecorated wooden desktop materials, higher density results in smaller contact temperature changes. A higher specific heat capacity results in lower contact temperature variation. A higher thermal conductivity results in a smaller contact temperature variation. A greater material thickness results in a smaller change in contact temperature. A higher room temperature results in a higher contact temperature.
4. After coating or veneering the desktop, the material's thermal conductivity properties change. The thickness, density, specific heat capacity, and thermal conductivity of the coating or veneer affect the final contact temperature. This clarifies the complex interaction pattern between the coating, veneer, and other decorative materials and the wood substrate's temperature sensation performance. In other words, wooden materials with high density, high specific heat capacity, and low thermal conductivity help maintain stable contact temperatures and enhance thermal comfort. Increasing thickness and applying appropriate decorative treatments (such as specific coatings or veneers) can slow down temperature fluctuations and improve user thermal comfort.
5. From a furniture design perspective, it is important to prioritize wood-based materials that are denser and have a higher specific heat capacity and lower thermal conductivity, such as MDF or multilayer solid wood panels, to slow temperature fluctuations and enhance tactile comfort. Avoid materials with excessively high thermal conductivity or

low heat capacity, especially for furniture intended for use in cold environments. When applying surface treatments to substrates, choose coatings with lower thermal conductivity (*e.g.*, acrylic varnish) to improve warmth perception in winter or in cold regions. To maintain a cool feel (*e.g.*, in summer or tropical regions), use veneer materials with a higher thermal conductivity (such as certain decorative papers or thin wood veneers). The thickness of finishes or veneers should be controlled to a range of 0.2 to 0.6 mm to balance aesthetics and thermal comfort. Essentially, combining materials can create personalized comfort systems that provide thermal comfort while reducing energy consumption.

6. This study provides furniture manufacturers and designers with a quantitative reference standard for material selection and process control. Optimizing material ratios and processing techniques can achieve a higher level of comfort and durability, as well as the best thermal sensation. Therefore, this study's value lies in providing furniture manufacturers with a scientific tool to optimize material selection and processing techniques, proactively avoiding minor thermal shocks that could affect comfort. This ensures exceptional tactile quality in product design from the outset. It also establishes a 'thermal sensation index' for furniture materials, helping consumers to intuitively select products that are suited to their environments. Subsequent research on furniture thermal comfort could be expanded to integrate with smart home systems. Integrating with desktop heating modules could enhance temperature control functionality and increase product value.

ACKNOWLEDGMENTS

This study was supported by a research grant from the Huaqiao University of Research Initiation Grant Program (Grant No. 24SKBS009).

REFERENCES CITED

Acheli, A., and Serhane, R. (2015). "Mechanical behavior simulation of MEMS-based cantilever beam using COMSOL multiphysics," *AIP Publishing LLC* 1653, article 020005. DOI: 10.1063/1.4914196

Amin, N. D. M., Akasah, Z. A., and Razzaly, W. (2015). "Architectural evaluation of thermal comfort: Sick building syndrome symptoms in engineering education laboratories," *Procedia - Social and Behavioral Sciences* 204, 19-28. DOI: 10.1016/j.sbspro.2015.08.105

Andras, A., Popescu, F. D., Radu, S. M., Pasculescu, D., Brinas, I., Radu, M. A., and Peagu, D. (2024). "Numerical simulation and modeling of mechano–electro–thermal behavior of electrical contact using COMSOL multiphysics," *Applied Sciences* 14(10), article 4026. DOI: 10.3390/app14104026

Azad, V. J., Li, C., Verba, C., Ideker, J. H., and Isgor, O. B. (2016). "A COMSOL-gems interface for modeling coupled reactive-transport geochemical processes," *Computers & Geosciences* 92, 79-89. DOI: 10.1016/j.cageo.2016.04.002

Bai, J., Li, Y., Jiang, S., and Guan, H. (2022). "Preparation of wood furniture cooling coatings based on phase change microcapsules and its performance study," *BioResources* 17(1), 1319-1337. DOI: 10.15376/biores.17.1.1319-1337

Bulcao, C. F., Frank, S. M., Raja, S. N., Tran, K. M., and Goldstein, D. S. (2016). "Relative contribution of core and skin temperatures to thermal comfort in humans," *Journal of Thermal Biology* 25(1-2), 147-150. DOI:10.1016/S0306-4565(99)00039-X

Cannon, F. R., and Denhartog, E. A. (2019). "Quantitative evaluation of mattresses using a thermal seat tester," *Journal of the Textile Institute* 110(9), 1352-1358. DOI: 10.1080/00405000.2019.1598315

Czajkowski, U., Olek, W., Weres, J., and Guzenda, R. (2016). "Thermal properties of wood-based panels: thermal conductivity identification with inverse modeling," *European Journal of Wood and Wood Products* 74(4), 577-584. DOI: 10.1007/s00107-016-1021-6

Du, H., Lian, Z. W., Lan, L., Lai, D. Y. (2023). "Application of statistical analysis of sample size: How many occupant responses are required for an indoor environmental quality (IEQ) field study," *Build. Simul* 16 (4), 577-588. DOI: 10.1007/s12273-022-0970-4

Ferrarin, M., and Ludwig, N. (2000). "Analysis of thermal properties of wheelchair cushions with thermography," *Medical & Biological Engineering & Computing* 38(1), 31-34. DOI: 10.1007/BF02344685

Gbenou, T. R. S., Fopah-Lele, A., Wang, K. J. (2022). "Macroscopic and microscopic investigations of low-temperature thermochemical heat storage reactors: A review," *Renewable & Sustainable Energy Reviews* 161, article 112152. DOI: 10.1016/j.rser.2022.112152

Hasebe, Y., Iriki, M., and Takahasi, K. (1995). "Usefulness of r-r interval and its variability in evaluation of thermal comfort," *International Journal of Biometeorology* 38(3), 116-121. DOI: 10.1007/BF01208486

Horikiri, K., Yao, Y., and Yao, J. (2015). "Numerical optimisation of thermal comfort improvement for indoor environment with occupants and furniture," *Energy and Buildings* 88, 303-315. DOI: 10.1016/j.enbuild.2014.12.015

Huang, G., Zhang, M., Montiel, D., Soundararajan, P., Wang, Y., Denney, J. J., Corrao, A. A., Khalifah, P. G., and Thornton, K. (2021). "Automated extraction of physical parameters from experimentally obtained thermal profiles using a machine learning approach," *Computational Materials Science* 194, article 110459. DOI: 10.1016/J.COMMATSCI.2021.110459

Huizenga, C., Zhang, H., Arens, E., and Wang, D. (2004). "Skin and core temperature response to partial- and whole-body heating and cooling," *Journal of Thermal Biology* 29(7-8), 549-558. DOI: 10.1016/j.jtherbio.2004.08.024

Ikei, H., Song, C., and Miyazaki, Y. (2017). "Physiological effects of wood on humans: A review," *Journal of Wood Science* 63(1), 1-23. DOI: 10.1007/s10086-016-1597-9

Laouadi, A. (2024). "Physiological indicators of thermal comfort: a comprehensive approach using the metabolic-based predicted mean vote index," *Buildings (2075-5309)* 14(12),3861. DOI: 10.3390/buildings14123861

Jue, B., and Huiyuan, G. (2022). "Study on thermal comfort of wood tabletop materials," *Wood Research* 67(2), 326-339. DOI: 10.37763/wr.1336-4561/67.2.326339

Julious, S. A., Campbell, M. J., and Walters, S. J. (2007). "Predicting where future means will lie based on the results of the current trial," *Contemporary Clinical Trials* 28(4), 352-357. DOI: 10.1016/j.cct.2007.01.010

Jumel, J., Lepoutre, F., Roger, J. P., Neuer, G., Cataldi, M., and Enguehart, F. (2003). "Microscopic thermal characterization of composites," *Review of Scientific Instruments* 74(1), 537-539. DOI: 10.1063/1.1524040

Li, S.-P. (2006). "The mesh transformation method and optimal finite element solutions," *Bit Numerical Mathematics* 46(1), 85-95. DOI: 10.1007/s10543-005-0040-1

Loredan, N. P., Lipovac, D., Jordan, S., Burnard, M. D., and Sarabon, N. (2022). "Thermal effusivity of different tabletop materials in relation to users' perception," *Applied Ergonomics* 100, article 103664. DOI: 10.1016/j.apergo.2021.103664

Nastase, I., Croitoru, C., and Lungu, C. (2016). "A questioning of the thermal sensation vote index based on questionnaire survey for real working environments," *Energy Procedia* 85, 366-374. DOI: 10.1016/j.egypro.2015.12.263

Neacsu, C., Tabacu, I., Ivanescu, M., and Vieru, I. (2017). "The evaluation of the overall thermal comfort inside a vehicle," *IOP Conference Series: Materials Science and Engineering* 252, article 012031. DOI: 10.1088/1757-899X/252/1/012031

Ozcelik, G., and Becerik-Gerber, B. (2018). "Benchmarking thermoception in virtual environments to physical environments for understanding human-building interactions," *Advanced Engineering Informatics* 36, 254-263. DOI: 10.1016/j.aei.2018.04.008

Parry, S., and Straker, L. (2013). "The contribution of office work to sedentary behaviour associated risk," *BMC Public Health* 13(1), article 296. DOI: 10.1186/1471-2458-13-296

Pérez-Aparicio, J. L., Palma, R., and Taylor, R. L. (2016). "Multiphysics and thermodynamic formulations for equilibrium and non-equilibrium interactions: Non-linear finite elements applied to multi-coupled active materials," *Archives of Computational Methods in Engineering* 23(3), 535-583. DOI: 10.1007/s11831-015-9149-9

Ramachandran, O., Kempel, L., Verboncoeur, J., and Shanker, B. (2023). "A necessarily incomplete review of electromagnetic finite element particle-in-cell methods," *IEEE Transactions on Plasma Science* 51(7), 1718-1728. DOI: 10.1109/tps.2023.3257165

Rawal, R., Garg, V., Kumar, S., and Adhvaryu, B. (2020). "Evaluation of thermally activated furniture on thermal comfort and energy consumption: An experimental study," *Energy and Buildings* 223(1), article 110154. DOI: 10.1016/j.enbuild.2020.110154

Rugh, J. P., Farrington, R. B., Bharathan, D., Vlahinos, A., Burke, R., Huizenga, C., Zhang, H., Rugh, J. P., and Farrington, R. B. (2004). "Predicting human thermal comfort in a transient nonuniform thermal environment," *European Journal of Applied Physiology* 92(6), 721-727. DOI: 10.1007/s00421-004-1125-2

Schweitzer, M. A. (2012). "Generalizations of the finite element method," *Open Mathematics* 10(1), 3-24. DOI: 10.2478/s11533-011-0112-1

Sung, W. T., Hsiao, S. J., Shih, J., A. (2019). "Construction of Indoor Thermal Comfort Environmental Monitoring System Based on the IoT Architecture," *Journal of Sensors* (1), article 2639787. DOI:10.1155/2019/2639787

Trim, S. J., Butler, S. L., and Spiteri, R. J. (2021). "Benchmarking multiphysics software for mantle convection," *Computers & Geosciences* 154(1), article 104797. DOI: 10.1016/j.cageo.2021.104797

Vlaović, Z., Domljan, D., and Grbac, I. (2012a). "Research of temperature and moisture during sitting on office chairs," *Drvna Industrija* 63, 105-112. DOI: 10.5552/drind.2012.1139

Vlaović, Z., Domljan, D., Župčić, I., and Grbac, I. (2012b). "Thermal comfort while sitting on office chairs – Subjective evaluations," *Drvna Industrija* 63(4), 263-270. DOI: 10.5552/drind.2012.1222

Wang, J. (2024). "Thermal comfort simulation in furniture design: integrating considerations of the building thermal environment," *International Journal of Heat & Technology* 42(2), 688-696. DOI: 10.18280/ijht.420236

Xiong, J., Lian, Z., Zhou, X., You, J., and Lin, Y. (2016). "Potential indicators for the effect of temperature steps on human health and thermal comfort," *Energy & Buildings* 113(2), 87-98. DOI: 10.1016/j.enbuild.2015.12.031

Yazid, A., Abdelkader, N., and Abdelmadjid, H. (2009). "A state-of-the-art review of the X-FEM for computational fracture mechanics," *Applied Mathematical Modelling* 33(12), 4269-4282. DOI: 10.1016/j.apm.2009.02.010

Younes, A., Ackerer, P., and Delay, F. (2010). "Mixed finite elements for solving 2-D diffusion-type equations," *Reviews of Geophysics* 48(1), article 277. DOI: 10.1029/2008RG000277

Yu, T., Jiang, F., Wang, C., Cao, M., Wang, Z., Chang, Y., and Guo, C. H. (2021). "Investigation on fabrication and microstructure of Ti-6Al-4V alloy hollow spheres by powder metallurgy," *Metals and Materials International* 27(5), 1083-1091. DOI: 10.1007/s12540-019-00462-5

Zhou, S., Rabczuk, T., and Zhuang, X. (2018). "Phase field modeling of quasi-static and dynamic crack propagation: COMSOL implementation and case studies," *Advances in Engineering Software* 122, 31-49. DOI: 10.1016/j.advengsoft.2018.03.012

Zhou, S., Zhuang, X., and Rabczuk, T. (2019). "Phase-field modeling of fluid-driven dynamic cracking in porous media," *Computer Methods in Applied Mechanics and Engineering* 350, 169-198. DOI: 10.1016/j.cma.2019.03.001

Article submitted: July 30, 2025; Peer review completed: September 16, 2025; Revised version received: October 1, 2025; Accepted: October 10, 2025; Published: October 28, 2025.
DOI: 10.15376/biores.20.4.10771-10794